First-principles studies for structural transitions in ordered phase of cubic approximant Cd_6Ca

2008 J. Phys.: Condens. Matter 20 315206

(http://iopscience.iop.org/0953-8984/20/31/315206)

J. Phys.: Condens. Matter **20** (2008) 315206 (9pp) doi:10.1088/0953-8984/20/31/315206

First-principles studies for structural transitions in ordered phase of cubic approximant Cd_6Ca

K Nozawa[1] **and Y Ishii**

Department of Physics, Chuo University, and SORST-JST, 1-13-27, Kasuga, Bunkyo-ku, Tokyo 112-8551, Japan

Received 16 April 2008, in final form 5 June 2008
Published 17 July 2008
Online at stacks.iop.org/JPhysCM/20/315206

Abstract

Recently a low-temperature structural transition has been reported for complex cubic compounds Cd_6M (M = Ca, Yb, Y, rare earth) and it is believed that the transition is due to orientational ordering of an atomic shell in the icosahedral cluster in Cd_6M. The first-principles electronic structure calculations and structural relaxations are carried out to investigate structures and orientational ordering of the innermost tetrahedral shell of the icosahedral cluster in Cd_6Ca. The very short interatomic distances in the experimental average structures are relaxed and the innermost tetrahedral shell of an almost regular shape is obtained. Three types of orientation for the tetrahedral shell and eight different combinations of them for the clusters at a vertex and body-centre of a cubic cell are obtained. A possible model describing the orientational ordering at low temperatures or high pressures is discussed.

(Some figures in this article are in colour only in the electronic version)

1. Introduction

Cubic Cd_6M (M = Yb, Ca) was recognized as an approximant crystal of binary quasicrystals $Cd_{5.7}M$ soon after the discovery of the quasicrystalline phase [1–4]. The crystal structure of Cd_6M is understood as a packing of four-layered atomic clusters with *glue* Cd atoms in the interstitial region between them. An anomalous temperature dependence of the electrical resistivity and specific heat was found for cubic Cd_6M near 100 K by Tamura *et al* [5]. The anomalies were attributed to orientational ordering of the innermost shell of the four-layered cluster [6, 7]. Watanuki *et al* [8] observed various phases under high pressure, where orientation of the innermost shell was assumed to be ordered differently. So far the transition has been observed only for cubic approximants but not for quasicrystals and cluster linkages in quasiperiodic structures seem to prevent the long-range orientational ordering of the innermost shell. It is certainly important to obtain a microscopic model of the orientational ordering, not only for elucidating the mechanism of the novel structural transition in inter-metallic compounds with complex structures but also for understanding mechanism of quasiperiodic ordering in Cd-based alloys.

The innermost atomic shell of the four-layered cluster, which is referred to as the first shell, is considered to be a tetrahedral Cd cluster [3, 9]. The second, third and fourth shells are a dodecahedron of twenty Cd atoms, an icosahedron of twelve M (=Ca,Yb) atoms and an icosidodecahedron of thirty Cd atoms, respectively. The four-layered cluster is illustrated in figure 1. At room temperature, the orientation of the first shell is randomly distributed and the crystal structure is treated as an average one with the space group symmetry $Im\bar{3}$. The four-layered clusters are placed at a vertex and a body-centre of a cubic unit cell and the total number of atoms in the unit cell is 168 including 36 glue atoms. In x-ray measurements at room temperatures, the first shell is described as a fractional site and so the structure and orientation of the first shells are open to argument.

According to Palenzona's analysis for the high-temperature phase, four atoms sit on eight vertices of a small cube with half occupancy at the centre of the clusters [3]. Because Cd atoms are not small enough to occupy neighbouring vertices of the cube, the first shell is reasonably assumed to be of a tetrahedral shape as shown in figure 2(a). The figure in the right panel of figure 2 is a schematic illustration of the first shells. Atoms

[1] Present address: Graduate School of Material Science, University of Hyogo, 3-2-1, Kouto, Kamigori, Hyogo, 678-1297, Japan.

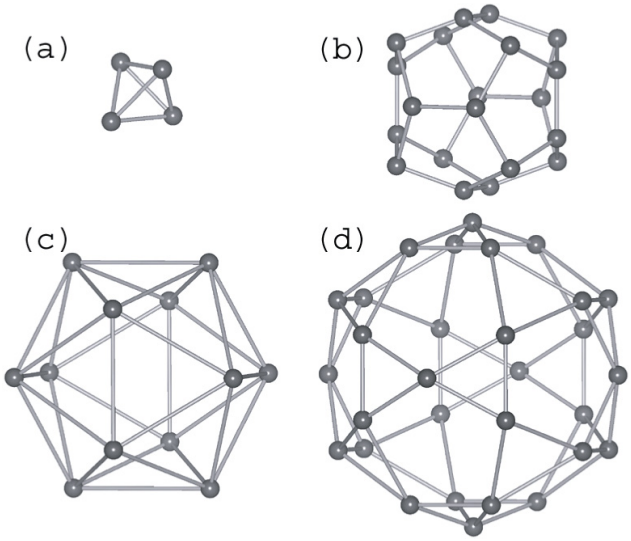

Figure 1. The four-layered atomic cluster of Cd_6Ca. The first, second, third and fourth shells correspond (a), (b), (c) and (d), respectively.

on vertices of a cube means that they are under the second shell's atoms on the three-fold axis of the cubic unit cell. Average structures obtained from experiments usually involve very short interatomic distances. Assuming the atomic structure of Cd_6M proposed by Palenzona as a starting one, we carried out first-principles structural relaxation and found that the first and second shells of the cluster are significantly distorted to avoid too short a Cd–Cd distance [10].

The tetrahedral shape of the first shell leads to a model of orientational ordering, in which two possible orientations of the tetrahedron are treated as Ising spin. Then the orientational ordering of the tetrahedral first shell is a phase transition of the Ising model on a body-centred-cubic lattice. An Ising-like ordering of the tetrahedral shells requires their rotation for orientational changes and then the energy cost is far larger than the thermal energy near the transition temperatures reported for ambient- and high-pressure phases [5, 8]. In fact, we have checked that the energy cost is more than 1 eV per cell when the tetrahedral first shell at the body-centre is rotated by 90° around the two-fold axis with the first shell at the vertex fixed. Widom and Mihalkovič arrived at a similar conclusion by Ising-model analysis for the transition temperature [11].

Gómez and Lidin proposed an alternative structural model for a high-temperature phase of Cd_6M, in which each vertex of the tetrahedron is replaced with triple split sites [9] (figure 2(b)). Atoms on the edges in the right panel imply that they are not under the atoms on the three-fold axis but are under the pentagonal faces of the second shell. Since the interatomic distances are longer than those in the regular tetrahedron of the Palenzona structure, this structural model may be more favourable than the Palenzona one. Moreover, the model seems suitable for describing orientational changes of the first shell because a rotation of the first shell is not needed for orientational change.

A similar transition has been found for isostructural Zn_6Sc [12]. Structural analyses for the high-temperature disordered phase [13] and the low-temperature ordered

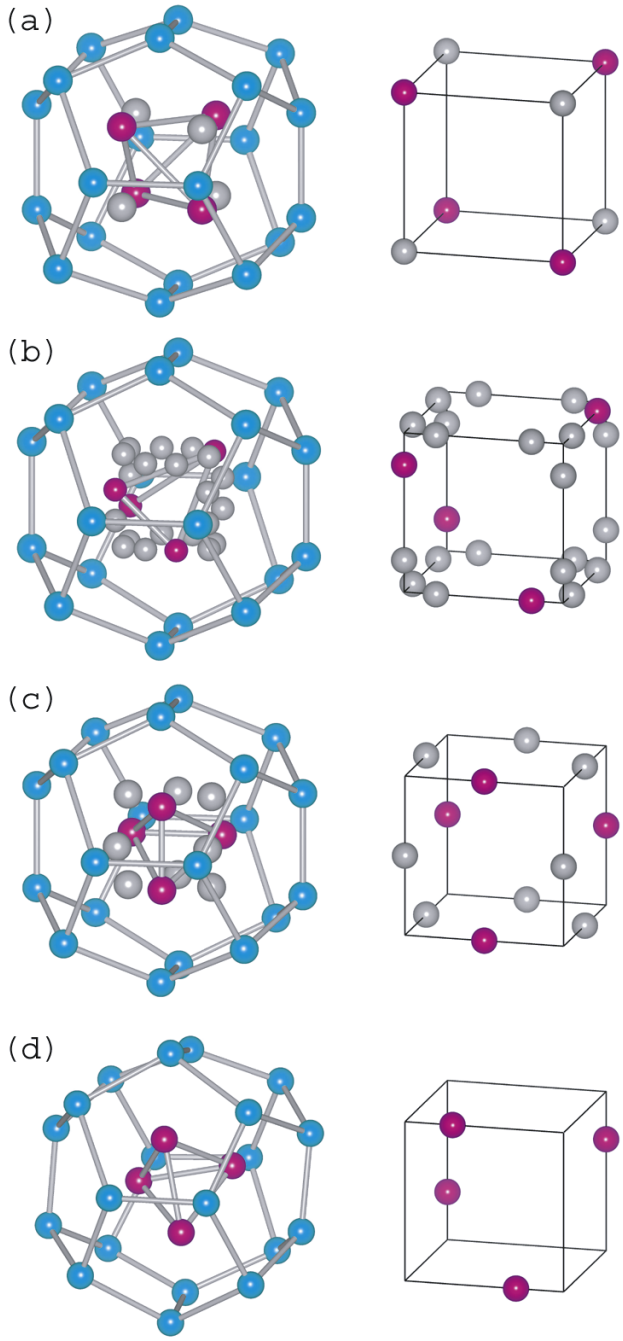

Figure 2. Schematic diagrams for experimentally proposed structures. (a) In the Palenzona model, four Cd atoms are sitting on the vertices of a small cube. A reasonable choice of occupied vertices forms a regular tetrahedron. (b) Each vertex of the small cube splits into triple sites and a Cd atom occupies the site with 1/6 occupancy in the Gómez–Lidin model. (c) The Lin–Corbett model is roughly interpreted as the 1/3 occupancy of the midpoint of the edges of the cube. A reasonable choice forms a tetrahedron, the two-fold axis of which corresponds to that of the outer dodecahedron. (d) One obtains the Ishimasa type tetrahedron by a rotation of the Lin–Corbett type tetrahedron around the two-fold axis. Note that the Ishimasa model has no fractional site, because it describes the ordered low-temperature phase.

one [14] have been reported. In the high-temperature phase, the 24g sites ($Im\bar{3}$) with 1/3 occupancy form a cuboctahedron as shown in figure 2(c). A reasonable choice of the fractional

sites is such that gives a tetrahedron

$$(x, y, 0), \quad (-x, y, 0), \quad (0, -x, -y), \quad (0, -x, y), \tag{1}$$

where $x = 0.0810$ and $y = 0.0748$, by Lin and Corbett [13]. A two-fold axis of the tetrahedron (the y-axis for the above choice) coincides with that of the outer dodecahedral shell and the cubic unit cell. We refer to this cluster structure as the Lin–Corbett structure hereafter. In the low-temperature structure, which is for an ordered phase with the space group symmetry $C2/2$, the tetrahedron is rotated slightly around the two-fold axis to avoid short distances between atoms in the first and second shells. The atomic positions in this structure are approximately reduced to those in a cubic cell as

$$(x, y, z), \quad (-x, y, -z), \quad (-z, -y, x), \quad (z, -y, -x), \tag{2}$$

with $x = 0.088$, $y = 0.064$ and $z = 0.018$. We refer to this cluster structure as the Ishimasa structure, which is illustrated in figure 2(d).

We reported results of a first-principles structural relaxation of cubic Cd_6Ca and discussed deformation of the inner atomic shells to relax the short interatomic distances in the experimental data [10, 15]. The previous calculations were, however, done with a single k-point, and more accurate estimates are needed for discussion of the optimal structure. Brommer *et al* performed a classical molecular-dynamics simulation using the potential energies determined by fitting to *ab initio* data, and found a phase transition near the experimentally reported transition temperature [16]. Although the obtained stable cluster is essentially that proposed by Ishimasa *et al* [14], a cluster orientation consistent with the experimental observation was not obtained. In addition, the previous works were done with a fixed lattice constant. The various ordered phases under pressure indicates the favourable structure depends on the lattice constant [8]. Calculations with different lattice constants are therefore required for discussing the phase diagram.

In this paper, we investigate the stable structure of the ordered phase of Cd_6M at several lattice constants using the Gómez–Lidin structure as the starting one for the first-principles structural relaxations.

2. Methods of calculations

First-principles calculations based on the density functional theory [17] are carried out within the local density approximation [18] to determine the stable structure and orientation of the first shells. The ultra-soft pseudo-potential technique [19] is used to represent the effective interaction between the valence electron and ionic core. The structural (ionic) relaxations are performed as a part of the first-principles calculations according to the force evaluated as the derivative of the total energy. Calculations have been performed using the *ab initio* total-energy and molecular-dynamics program VASP (Vienna *ab initio* simulation package) developed at the Institut für Materialphysik of the Universität Wien [20–23].

Cd_6Yb and Cd_6Ca show similar behaviour about the phase transition and we study Cd_6Ca in this paper. This is because Ca is easier to treat in the first-principles calculation than Yb with a localized f-state. The Cd 4d states are treated as valence states whereas a shallow semicore state of Ca 3p is treated as frozen core. Electron–electron interactions are treated within the local density approximation in the density functional theory and the exchange–correlation energy parameterized by Perdew and Zunger is used [24]. A cubic cell including two four-layered icosahedral atomic clusters and 36 glue Cd atoms is adopted as a unit cell in all calculations.

The wavefunctions are expanded with a plane-waves basis set up to a kinetic energy cutoff of 168 eV and Kohn–Sham equations are solved iteratively to optimize the electronic structure. The Brillouin zone is sampled with 14 irreducible k-points (Monkhorst–Pack $3 \times 3 \times 3$ grids). The numerical error due to the k-point sampling and the plane-wave cutoff is estimated by comparing with the results of more accurate calculations using 63 irreducible k-points ($5 \times 5 \times 5$ mesh) or 220 eV of plane-wave cutoff. The estimated error is of the order of 10 meV for the energy separation of different structures at the same lattice constant, while it is 60–80 meV for different lattice constants.

3. Results and discussion

3.1. Preparations for structural relaxations

In this section, we describe the starting structures for structural relaxations. According to the analysis by Gómez and Lidin for the high-temperature phase of Cd_6Ca [9], the 48h Wyckoff sites for $Im\bar{3}$ are occupied by Cd with 1/6 probability where coordinates are given as

$$x = 0.080\,61, \quad y = 0.074\,61, \quad z = 0.026\,87.$$

This structure is interpreted as that each of the four vertices of the regular tetrahedron split into triple sites, which are occupied with 1/3 occupancy. Therefore the number of possible structures of the first shell is 81 ($=3^4$). Most of these configurations are, however, equivalent. The 81 structures are classified into nine inequivalent structures shown in figure 3, where the grey and white balls denote the occupied and unoccupied sites, respectively. The number of equivalent structures in each group and the six interatomic distances in the first shell are listed in table 1.

The total energy of each structure is calculated with a cubic unit cell, in which the two identical icosahedral clusters are placed at vertex and body-centre. Since the structure except for the first shell is identical in each calculation, the difference in the total energies can be a measure of the relative stability of the first shell. We find that the group (i) in figure 3 is the most stable structure. The total energies presented in table 1 may involve a numerical error of the order of 10 meV per cell. However, since the difference in the energies between the most and second most stable structures is 1.1 eV per cell, the numerical error does not influence our conclusion. We note here that differences in the total energies shown in table 1 originate from differences in interatomic distances between

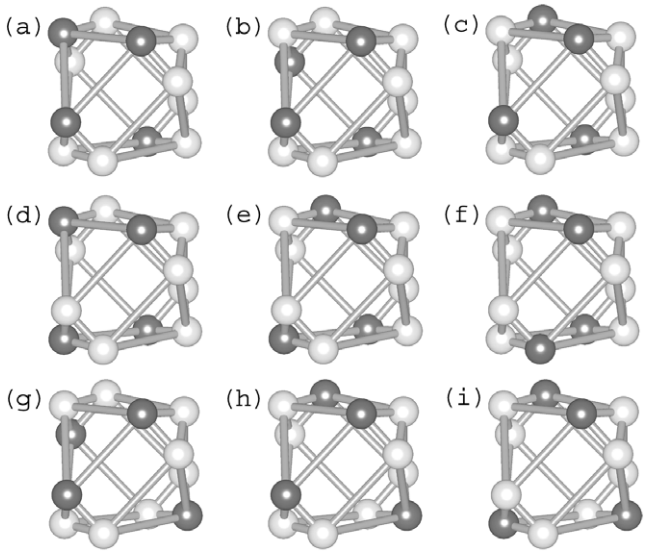

Figure 3. The nine symmetry inequivalent groups of the first shell. One of the triple split sites is occupied by Cd atoms (grey) and the others are vacancies (white).

Table 1. Nine inequivalent structures of the Gómez–Lidin clusters: multiplicity (the number of equivalent configurations), interatomic distances and relative total energies are shown.

Groups	Multiplicity	Interatomic distances in the first shell (Å)						Energy (eV)
a	12	2.32	2.32	2.32	3.03	3.06	3.45	4.8
b	6	2.32	2.32	2.67	3.03	3.03	3.45	3.0
c	12	2.32	2.49	2.67	3.03	3.06	3.45	1.9
d	6	2.32	2.32	2.49	3.06	3.06	3.45	3.5
e	12	2.32	2.49	2.67	3.03	3.06	3.45	1.9
f	3	2.49	2.49	2.67	2.67	3.45	3.45	1.1
g	12	2.32	2.67	3.03	3.03	3.03	3.06	1.1
h	12	2.32	2.49	3.03	3.06	3.06	3.06	1.6
i	6	2.49	2.67	3.03	3.03	3.06	3.06	0.0

atoms in the first shell because those between atoms in the first and other shells are identical for all the structures in figure 3. For the most stable structure group (i), very short Cd–Cd distances are avoided and the six interatomic distances are close to the nearest neighbour distance, 2.98 Å, in hexagonal-close-packed Cd [25].

The six symmetry-related structures of the group (i) are shown in figure 4 and their atomic coordinates are given as

$$
\begin{aligned}
&1\text{: } (-x,-y,-z), \quad (-x,y,z), \quad (y,z,-x), \quad (y,-z,x),\\
&2\text{: } (-y,-z,-x), \quad (-y,z,x), \quad (x,y,-z), \quad (x,-y,z),\\
&3\text{: } (-x,-y,-z), \quad (x,-y,z), \quad (-z,x,y), \quad (z,x,-y),\\
&4\text{: } (x,y,-z), \quad (-x,y,z), \quad (z,-x,y), \quad (-z,-x,-y),\\
&5\text{: } (-y,-z,-x), \quad (y,z,-x), \quad (-z,x,y), \quad (-z,-x,y),
\end{aligned}
\tag{3}
$$

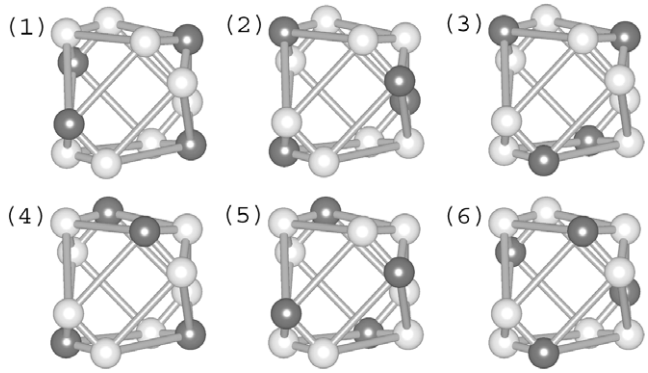

Figure 4. The symmetry equivalent structures of group (i) of figure 3. White spheres stand for vacancies. These six structures are isostructural, but face to different directions.

$$
6\text{: } (y,-z,x), \quad (-y,z,x), \quad (-z,-x,-y), \quad (z,x,-y).
$$

These structures are equivalent and related to each other by appropriate symmetry operations. The structure 1 is invariant under two-fold rotation around the x axis. The structure 2 is derived from 1 by two-fold rotation around either the y or z axis. The structures 3–6 are obtained by three-fold rotation of 1.

We construct the starting structures using the above stable clusters (i). Although different unit cells are proposed for Cd–Ca [26, 27] and Cd–Eu [28] systems, we consider here only the cubic unit cell with two four-layered icosahedral clusters at a vertex and body-centre. As mentioned above, the most stable structures of the first shell, the group (i), has six symmetry-related structures shown in figure 4. Accordingly, if one fixes the orientation of the first shell at the vertex of the cubic unit cell, the possible orientation of that at the body-centre is one of the six variants in the group (i) and those obtained by the space-inversion of the group (i). The 12 configurations are also classified into six inequivalent ones. They can be denoted using the symbols in figure 4 as 1–1, 1–2, 1–3, 1–1*, 1–2* and 1–3*. Here, X^* means the space-inversion of structure X. For instance, 1–2* is the combination of structure 1 and the space-inversion of structure 2.

3.2. Structural relaxations

After the relaxation, we find three types of clusters and eight crystal structures as combinations of the obtained clusters. Among three types of clusters, two of them are similar to the experimentally proposed ones: the Lin–Corbett (LC) [13] and the Ishimasa (IS) [14] types of structures. In both the LC and IS structures, the relaxed positions of atoms in the first shell are in the direction of the pentagonal faces of the dodecahedral second shell to avoid short distances between atoms in the first and second shells. Another type of cluster is that never proposed before: one atom is exactly on the three-fold axis of the outer dodecahedral shell and the cubic unit cell. A tetrahedron is rotated slightly around the three-fold axis and the atoms which are not on the three-fold axis are almost in the five-fold direction of the dodecahedral shell, $(1, \tau, 0)$ where

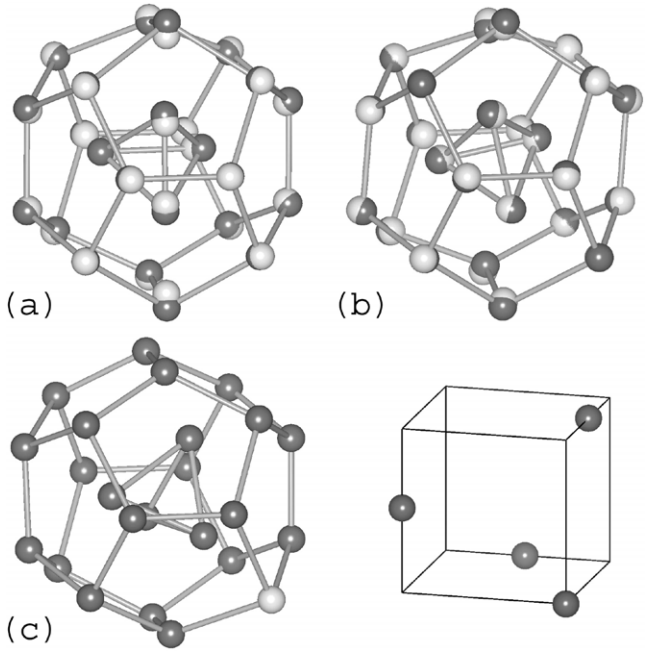

Figure 5. (a) Comparison of the Lin–Corbett structure (white) and the calculated cluster (grey). (b) Another type of the relaxed cluster (grey) and the Ishimasa structure (white). (c) The MT structure, which is different from any previously proposed structures. One atom of the first shell is on the three-fold axis of the cubic unit cell, whereas the remaining three atoms are under the pentagonal faces of the second shell. The white ball in the second shell denotes the atom, under which the atom of the first shell on the three-fold axis is placed.

τ is the golden mean. Because the first shell's atom on the three-fold axis is capped by a pyramid of atoms in the second shell, we refer to the new cluster as a mono-capped tetrahedron (MT) in this paper. The clusters obtained are compared with experimental ones in figure 5. In figures 5(a) and (b), the grey balls denote the obtained cluster and white balls represent the experimental ones. In the right panel of figure 5(c), a similar illustration to those in figure 2 is given for the MT-type for comparison.

The coordinates of the first-shell atoms are summarized in table 2. If one chooses a subset of the fractional sites to describe a tetrahedral shell as in (1) and (3), the tetrahedron is distorted and a centre of mass of four vertices is shifted from the symmetry centre. This is not the case for the Ishimasa structure (2). In the relaxed structures, the distortion of the tetrahedral shell is removed and the centre of mass of the tetrahedral cluster is almost at the symmetry centre. The interatomic distances in the first shell are $(2.76, 2.83, 2.92 \times 4)$ for the LC-type structures ($a = 15.3$ Å), $(2.83 \times 3, 2.91 \times 3)$ for the MT-type structures ($a = 15.3$ Å) and $(2.75, 2.80, 2.86 \times 2, 2.89 \times 2)$ for the IS structures ($a = 15.1$ Å).

Depending on the starting structures assumed, we obtain eight inequivalent crystal structures, in which the clusters at the vertex and body-centre are of the same type but their orientation is different. Two types of crystal structures with the LC-type clusters are obtained. One has LC-type clusters of the same orientation at the vertex and body-centre of the unit cell and the other has a LC-type cluster at the body-centre which is an inversion of that at the vertex. We refer to these structures as LC(E) and LC(I) ones. If the LC-type cluster rotates around its two-fold axis, the IS-type cluster is obtained. For the IS-type clusters, we obtain four different structures: (1) the IS-clusters at the vertex and body-centre have the same orientation (IS(E)), (2) the IS cluster at the body-centre is obtained by a two-fold rotation of that at the vertex (IS(2)) where the two-fold rotation is made around an axis perpendicular to the two-fold symmetry axis of the cluster, (3) the IS cluster at the body-centre is an inversion of the other (IS(I)), and (4) the IS-cluster at the body-centre is a mirror image of the other (IS(σ)). The IS(E) and IS(σ) structures are obtained from the LC(E) by rotating the first shell around the two-fold axis whereas the IS(I) and IS(2) ones are obtained from the LC(I). Therefore the four inequivalent IS structures are classified by combinations of the orientation and the rotation direction of the LC-cluster. Finally, two types of orientational combination of the MT-clusters are obtained where the tetrahedra are related by a two-fold rotation in the MT(2) structure and an inversion in the MT(I) structure.

We turn our discussion to the stability of the structures. The structural relaxations are performed at several lattice constants to obtain the equilibrium volume. We have checked the accuracy of the total energies for different lattice constants by changing a cutoff energy. The optimal lattice constants are around 15.3 Å for all the structures and shorter than the experimental ones at room temperatures by about 2.5%. Since a decrease of the lattice constant by thermal expansion is less than 1% for a temperature difference about 300 K [7, 27], this discrepancy is partly because of an error due to the local density approximation. Although the low-temperature phase of Cd_6M is analysed as a superstructure with a larger unit cell, we suppose that the LC, IS and MT-clusters are reasonable candidates for describing the orientational ordering.

The calculated total energies are shown in table 3. The energies are presented as differences from the most stable structure (the LC(I) structure at $a = 15.3$ Å). Note that a symbol '-' indicates that the structure is unstable and relaxes to a different one. For instance, IS(2) and IS(I) transform to the LC(I) structure at 15.3 Å. The relative stability depends not only on the structures of the clusters but also on their orientation. For instance, the LC(I) structure is the most stable one in a wide range of lattice constants but the LC(E) structure, which is locally identical with the LC(I) structure, takes the highest energy among the obtained structures. This indicates the importance of the cluster–cluster interactions. The most stable structure depends on the lattice constant. At larger lattice constants than the equilibrium ones, the MT structure is stable whereas the IS structure becomes more stable at $a = 15.1$ Å or smaller. It is also interesting to note that the total energies for the MT structures with different orientations of the clusters are essentially the same.

In the LC structure, the relaxed positions of atoms in the first shell are in the direction of the pentagonal faces of the dodecahedral second shell. In figure 6(a), we show the faces of the dodecahedral shell, under which the atoms in the tetrahedral first shell is placed, as coloured ones. When one chooses four faces separated as far as possible from

Table 2. Coordinates of atoms in the first shell.

	x	y	z
Gómez–Lidin [9]	0.0806	0.0746	0.0269
Lin–Corbett [13]	0.0810	0.0748	0
Ishimasa [14]	0.088	0.064	0.018
(translated to the	−0.088	0.064	−0.018
cubic lattice)	−0.022	−0.067	0.090
	0.022	−0.067	−0.090

	Vertex			Body-centre $+(\frac{1}{2}, \frac{1}{2}, \frac{1}{2})$		
	x	y	z	x	y	z
LC(E)	0.090	0.075	0.001	−0.090	0.075	−0.001
	−0.090	0.075	−0.001	0.090	0.075	0.001
	0.000	−0.066	−0.093	0.000	−0.066	−0.093
	0.000	−0.066	0.093	0.000	−0.066	0.093
LC(I)	0.090	0.073	0.002	−0.090	−0.073	0.002
	−0.090	0.073	−0.002	0.090	−0.073	−0.002
	0.002	−0.068	−0.092	−0.002	0.068	−0.092
	−0.002	−0.068	0.092	0.002	0.068	0.092
MT(2)	0.095	0.011	0.059	−0.095	−0.011	0.059
	−0.060	0.095	−0.013	0.059	−0.095	−0.013
	0.013	−0.060	−0.096	−0.013	0.060	−0.096
	−0.071	−0.070	0.068	0.071	0.070	0.068
MT(I)	0.015	0.061	−0.095	0.061	0.095	0.015
	0.095	−0.015	0.061	−0.095	0.015	−0.061
	−0.061	−0.095	−0.015	−0.015	−0.061	0.095
	−0.069	0.069	0.069	0.069	−0.070	−0.069
IS(2)	0.089	0.071	0.019	−0.089	−0.071	0.019
	−0.089	0.071	−0.019	0.089	−0.071	−0.019
	−0.018	−0.068	0.091	0.018	0.068	0.091
	0.018	−0.068	−0.091	−0.018	0.068	−0.091
IS(I)	0.089	−0.070	0.018	−0.089	0.070	−0.018
	−0.089	−0.070	−0.018	0.089	0.070	0.018
	0.016	0.069	−0.091	−0.016	−0.069	0.091
	−0.016	0.069	0.091	0.016	−0.069	−0.091
IS(E)	−0.017	−0.066	0.091	−0.016	−0.066	0.091
	0.017	−0.066	−0.091	0.017	−0.066	−0.091
	−0.089	0.073	−0.017	−0.089	0.073	−0.017
	0.089	0.073	0.017	0.089	0.073	0.017
IS(σ)	0.031	0.065	−0.088	−0.031	0.065	−0.088
	−0.031	0.065	0.088	0.031	0.065	0.088
	0.086	−0.071	0.032	−0.086	−0.071	0.032
	−0.086	−0.071	−0.032	0.086	−0.071	−0.032

Table 3. Relative total energies (eV) after the structural relaxations. Asterisks represent the optimal energy at each lattice constant. A symbol '—' indicates that the structure is unstable.

a	LC(E)	LC(I)	MT(2)	MT(I)	IS(2)	IS(I)	IS(E)	IS(σ)
15.7	4.854	4.819	4.724*	4.727	—	—	—	—
15.5	1.522	1.470	1.435*	1.440	—	—	—	—
15.4	0.536	0.471*	0.476	0.479	—	—	—	—
15.3	0.082	0.000*	0.047	0.052	—	—	—	—
15.1	0.819	0.700	—	0.808	0.695*	0.713	0.820	0.799
14.9	4.121	3.957	—	4.126	3.929*	3.966	4.092	4.056

12 pentagonal faces of the dodecahedral second shell, one inevitably has faces sharing an edge. A blue (or dark grey in greyscale) face in figure 6(a) is a face sharing an edge with the other whereas a yellow (or light grey) one is a separated one. The coordinate of the atom in the first shell under the yellow face is $(0.002, -0.068, \pm 0.092)$, which is close to the five-fold direction $(0, -1, \pm\tau)$, whereas the atom under the blue face is at $(\pm 0.090, -0.073, 0.002)$ and shifted from the five-fold direction to the green (or grey) site in the dodecahedral shell. Consequently the green sites are moved outward to a position on a triangular face of the icosahedral third shell. In the IS structure, the distortion of the second shell is slightly smaller because the rotation of the first shell around the two-fold axis relaxes the repulsive interaction between atoms in the first and second shells.

In figure 6(b), we show the charge densities of the LC(I) structures on the (001) plane for states in the energy range from −1.0 to −0.5 eV below the Fermi energy. The red, blue, green and grey balls in the figure denote the atoms of the first, second, third and fourth shells, respectively. The green sites in figure 6(a) and characteristic charge clouds around them are indicated by black arrows. Such charge clouds are

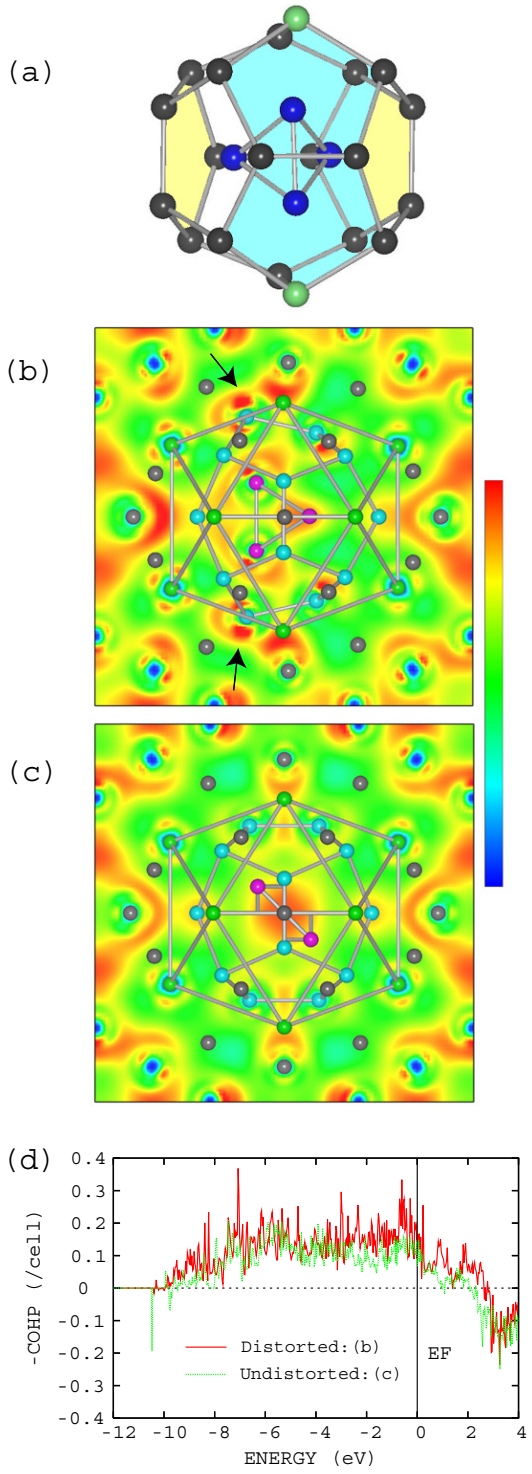

Figure 6. (a) The LC-type cluster. The coloured pentagonal faces indicate those having the first-shell atoms under themselves. The blue faces are those sharing an edge and the yellow ones are separated ones. The green site represents the atom which is close to the atom in the first shell. Charge density plots on the (001) plane including (b) the distorted area of the LC structure and (c) the corresponding area of the non-distorted second shell with Palenzona's core. The charge densities are summed over the energy range from −1.0 to −0.5 eV. Black arrows indicate characteristic charge clouds near the significantly distorted site. (d) The crystal orbital Hamilton population between the displaced second shell's atom and the fourth shell's atom located near the second shell's atom. The significant increase in the −COHP of the LC structure imply an increase of Cd–Cd bonding.

not seen around the undistorted second shell in the Palenzona model (figure 6(c)). Figure 6(d) shows the crystal orbital Hamilton population (COHP) [29] between the significantly distorted green sites in figure 6(a) and the neighbouring atoms in the fourth shell. The calculation is made with the tight-binding linear muffin-tin orbitals method in the atomic-sphere approximation [30]. The red (solid) curve represents the COHP of the (relaxed) LC(I) structure and the green (dotted) one is for the unrelaxed structure of the Palenzona model. Note that we plot the COHP multiplied −1 in the figure. Positive values below the Fermi energy imply the bonding trend between the atoms. One can find the bonding trend increases for the states around −1 eV for the relaxed structure. Therefore the characteristic charge clouds in figure 6(b) are a signature of increasing Cd–Cd bonding induced by the distortion of the second shell.

The IS-type structures, which is obtained by rotating the first shell in the LC-type structure around the two-fold axis, become stable at lattice constants smaller than the equilibrium one. We suppose that the rotation relaxes the repulsive interaction between atoms in the first and second shells for smaller lattice constants. Because the LC(I) structure is more stable than the IS-type structure at $a = 15.3$ Å, it is reasonably assumed that the potential energy surface (PES) with respect to the rotation angle of the first shell around the two-fold axis has a single minimum as shown in figure 7(a). In the figure, total energies for unstable structures are evaluated with the rotation angle fixed. The solid line is obtained by cubic spline interpolation. At $a = 15.1$ Å, the IS(2) becomes slightly more stable than the LC(I) structure where the energy difference is about 5 meV (50 K), which is as small as the numerical error involved in the present calculation. Then the PES with respect to the rotation angle have shallow double minima for $a = 15.1$ Å as is shown schematically in figure 7(b). The rotation of the first shell is expected to be allowed above 50 K.

Watanuki *et al* reported various ordered phases in Cd_6Yb at high pressure [8]. The ordered phase, which is stable at ambient pressure and low temperature (phase I), transforms to phase III at 1 GPa. The compression ratio of the lattice constants at ambient and transition pressure is about 1% [31]. By heating, the phase III transforms to phase II at about 130 K via phase III', which exists in the temperature range about 100–130 K. We speculate that the IS-type structure is stabilized under high pressure whereas the LC-type one is stable at ambient pressure for Cd_6Ca. A ratio of the lattice constants (15.1/15.3) coincides with the experimental compression ratio of the lattice constant at the transition from the phase I to III. Using a volume change by compression ΔV and $p = 1$ GPa, we evaluate $p\Delta V$ as 0.87 eV/cell, which is comparable to the energy difference, 0.70 eV/cell, between LC(I) at 15.3 Å and IS(2) at 15.1 Å. This implies that the transition from the LC structure to the IS one can take place under the pressure around 1 GPa.

The transition temperature from the phase III to III' (about 100 K) is also close to the temperature at which the cluster rotation is allowed (50 K). Moreover, the energy difference between IS(2) and IS(I) structures at $a = 15.1$ Å is about 180 K, which is close to the transition temperature from the

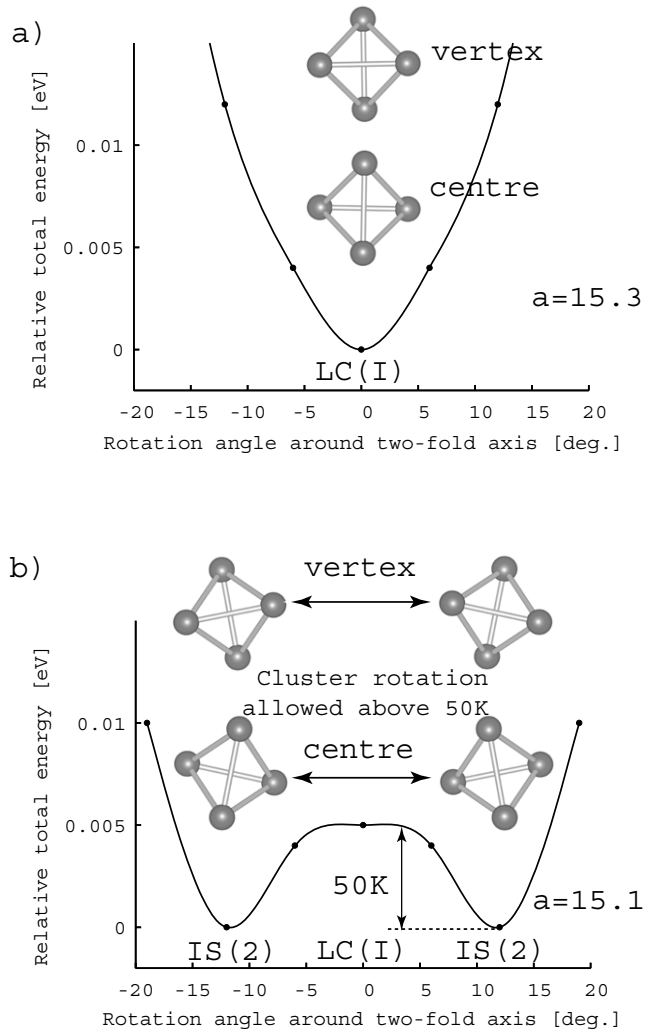

Figure 7. Potential energy surface (PES) with respect to the rotation angle θ of the first shell around its two-fold axis. (a) At the equilibrium lattice constant $a = 15.3$ Å, the LC(I) structure is most stable. It implies that the PES has a minimum at $\theta = 0$. (b) At $a = 15.1$ Å or smaller, the IS(2) structure becomes the most stable. Consequently, the PES has two minima at $\theta \neq 0$.

phase III' to II. Above 180 K, the cluster rotations at the vertex and body-centre are expected to take place independently because the thermal energy overcomes the energy difference between IS(2) and IS(I). From these results, we speculate that phase III is an ordered phase with the IS-type first shell and the transitions to phase III' and II are induced by the cluster rotation of the first shell around the two-fold axis. Brommer *et al* obtained the IS-type cluster as a stable one by a classical molecular-dynamics simulation, and found a phase transition at 89 K [16]. Although the crystal structure (orientational configurations of clusters) of the ground state is not determined, the reported structure of the stable cluster is similar to the present result at 15.1 Å and the low transition temperature is consistent with the proposed PES in figure 7(b). The predicted transition by Brommer *et al* therefore might be concerned with the cluster rotation around the two-fold axis as shown in figure 7(b). At $a = 14.9$ Å, the energy difference between the optimal IS(2) and the others increases. This seems consistent with an increase of the transition temperature with increasing pressure [8].

In the 1/1 cubic approximant, two types of linkages between the clusters are realized: one is the two-fold one corresponding to an edge of the unit cell and the other is the three-fold one connecting the vertex and body-centre. These linkages in cubic Cd_6Ca are parallel to the two-fold axis of the LC- and IS-clusters and the three-fold one of the MT-cluster. Takakura *et al* [32] pointed out the significance of the cluster linkage in the atomic structure of the icosahedral Cd–Yb quasicrystal. Besides the (100) and (111) directions, there are other two- and three-fold directions of the linkages in icosahedral quasicrystals. If the orientation of the tetrahedral shell correlates with that of the cluster linkage, the quasiperiodic arrangement of the clusters may prevent the orientational ordering of the tetrahedral shell.

4. Summary and conclusion

First-principles structural relaxations are carried out for the 1/1 cubic approximant Cd_6Ca. The very short interatomic distances in the experimental average structures are relaxed and the innermost tetrahedral shell of an almost regular shape is obtained. Three types of orientation of the tetrahedral shell relative to the second shell are found: the LC-type, IS-type and newly found MT-type. Although the low-temperature phase of Cd_6Ca is analysed as a superstructure with a larger unit cell, we presume that three types of orientation of the tetrahedral shell obtained here are reasonable candidates for describing the orientational ordering.

Depending on the starting structures assumed, we obtain eight inequivalent crystal structures, in which the clusters at a vertex and body-centre are of the same type but their orientation is different. At the equilibrium lattice constant, the LC(I) structure is the most stable. When the lattice constant decreases, the IS(2) structure, which is obtained by rotating the first shell in the LC(I) structure around the two-fold axis, becomes the most stable one. It is supposed that the rotation of the first shell relaxes the repulsive interaction between atoms in the first and second shells for a smaller lattice constant. The pressure-induced structural transitions observed by Watanuki *et al* are discussed in connection with the structural change between the LC and IS structures.

The IS-type structure is essentially the same as that obtained by Ishimasa *et al* for the low-temperature ordered phase of Zn_6Sc [14]. In the present calculation for Cd_6Ca, the LC structure is obtained as the most stable one at the equilibrium lattice constant and the IS one becomes the most stable for shorter lattice constants. As we stressed here, the IS structure is derived from the LC one by rotating the first shell around its two-fold axis. We conclude that the LC-cluster and its rotation could provide a plausible model for the orientational ordering in the complex cubic Cd_6M and Zn_6Sc.

Acknowledgments

The authors would like to thank K Makoshi, N Shima, T Fujiwara, M Krajčí, R Tamura, T Watanuki, T Ishimasa,

M Widom and M Mihalkovič for useful discussion. Figures of crystal structure and charge density in this paper are drawn by VESTA as developed by K Momma and F Izumi [33]. This work is partly supported by Solution Oriented Research for Science and Technology, Japan Science and Technology Agency.

References

[1] Guo J Q, Abe E and Tsai A P 2000 *Phys. Rev.* B **62** R14605
[2] Tsai A P, Guo J Q, Abe E, Takakura H and Sato T J 2000 *Nature* **408** 538
[3] Palenzona A 1971 *J. Less-Common Met.* **25** 367
[4] Takakura H, Guo J Q and Tsai A P 2001 *Phil. Mag. Lett.* **81** 411
[5] Tamura R, Murao Y, Takeuchi S, Tokiwa K, Watanabe T, Sato T J and Tsai A P 2001 *Japan. J. Appl. Phys.* **40** L912
[6] Tamura R, Murao Y, Takeuchi S, Ichihara M, Isobe M and Ueda Y 2002 *Japan. J. Appl. Phys.* **41** L524
[7] Tamura R, Edagawa K, Aoki C, Takeuchi S and Suzuki K 2003 *Phys. Rev.* B **68** 174105
[8] Watanuki T, Machida A, Ikeda T, Aoki K, Kaneko H, Shobu T, Sato T J and Tsai A P 2006 *Phys. Rev. Lett.* **96** 105702
[9] Gómez C P and Lidin S 2003 *Phys. Rev.* B **68** 024203
[10] Nozawa K and Ishii Y 2004 *MRS Symp. Proc. (Boston)* vol 805 (Warrendale: Material Research Society) p 47
[11] Widom M and Mihalkovič M 2004 *MRS Symp. Proc. (Boston)* vol 805 (Warrendale: Material Research Society) p 53
[12] Tamura R, Nishimoto K, Takeuchi S, Edagawa K, Isobe M and Ueda Y 2005 *Phys. Rev.* B **71** 92203
[13] Lin Q and Corbett J D 2004 *Inorg. Chem.* **43** 1912
[14] Ishimasa T, Kasano Y, Tachibana A, Kashimoto S and Osaka K 2007 *Phil. Mag.* **87** 2887
[15] Nozawa K and Ishii Y 2006 *Phil. Mag.* **86** 615
[16] Brommer P, Gähler F and Mihalkovič M 2007 *Phil. Mag.* **87** 2671
[17] Hohenberg P and Kohn W 1964 *Phys. Rev.* **136** B864
[18] Kohn W and Sham L J 1965 *Phys. Rev.* **140** A1133
[19] Vanderbilt D 1990 *Phys. Rev.* B **41** 7892
[20] Kresse G and Hafner J 1993 *Phys. Rev.* B **47** 558
Kresse G and Hafner J 1994 *Phys. Rev.* B **49** 14251
[21] Kresse G and Furthmüller J 1996 *Comput. Mater. Sci.* **6** 15
[22] Kresse G and Furthmüller J 1996 *Phys. Rev.* B **54** 11 169
[23] Kresse G and Hafner J 1994 *J. Phys.: Condens. Matter* **6** 8245
[24] Perdew J P and Zunger A 1981 *Phys. Rev.* B **23** 5048
[25] Bruzzone G and Merlo F 1973 *J. Less-Comm. Met.* **30** 303
[26] Gómez C P and Lidin S 2001 *Angew. Chem.* **113** 4161
[27] Tamura R, Edagawa K, Shibata K, Nishimoto K, Takeuchi S, Saitoh K, Isobe M and Ueda Y 2005 *Phys. Rev.* B **72** 174211
[28] Gómez C P and Lidin S 2004 *Chem. Eur. J.* **10** 3279
[29] Dronskowski R and Blöchl P E 1993 *J. Phys. Chem.* **97** 8617
[30] Andersen O K, Jepsen O and Glötzel D 1985 *Highlights of Condensed Matter Theory* ed F Bassani, F Fumi and M P Tosi (New York: North-Holland) p 59
[31] Watanuki T 2007 private communication
[32] Takakura H, Gómez C P, Yamamoto A, de Boissieu M and Tsai A P 2007 *Nat. Mater.* **6** 58
[33] Momma K and Izumi F 2008 *J. Appl. Crystallogr.* **41** 653